High-fidelity predictive integrated modeling of the high power (steady-state) plasma in the Volumetric Neutron Source (VNS) tokamak

E. Bray[1]*, C. Bourdelle[2], C. Angioni[3], E. Fable[3], D. Fajardo[3], Ph. Lauber[3], T. Luda[3], C. Marchetto[1], M. Marin[4], M. Maslov[5], F.Maviglia[6,7], L.Pigatto[8] A. Quartararo[9], M. Siccinio[3,6], F. Subba[1], G. Tardini[3], M. Weiland[3], S. Wiesen[10]

[1]NEMO Group, Dipartimento Energia, Politecnico di Torino, Corso Duca degli Abruzzi 24, 10129 Torino, Italy.
[2]CEA, IRFM, F-13108 Saint-Paul-lez-Durance, France.
[3]Max–Planck–Institut für Plasmaphysik, Boltzmannstrasse 2, D–85748 Garching, Germany.
[4] SPC, Swiss Plasma Center, Ecole Polytechnique Federale de Lausanne, Station 13, Lausanne 1015, Switzerland
[5]UKAEA, Culham Science Centre, Abingdon OX143DB, United Kingdom of Great Britain and Northern Ireland
[6] EUROfusion – Programme Management Unit, Boltzmannstrasse 2, 85748 Garching, Germany
[7] Associazione EURATOM-ENEA sulla Fusione, C.R. Frascati, C.P. 65-00044 Frascati, Rome, Italy
[8] Consorzio RFX, Corso Stati Uniti 4, 35127 Padova, Italy
[9] Department of Engineering, University of Palermo, Viale delle Scienze, 90128 Palermo, PA, Italy
[10] DIFFER—Dutch Institute for Fundamental Energy Research, De Zaale 20, 5612 AJ Eindhoven, Netherlands

Abstract

The development of a Volumetric Neutron Source (VNS) is crucial for testing in-vessel components under full nuclear fusion environments. The beam-driven VNS requires steady-state operational qualification targeting high neutron wall-loading of NWL = 0.5 MW/m^2. This work presents a self-consistent high-fidelity 1.5D integrated modeling framework using the ASTRA code coupled with the TGLF-SAT2 transport solver and RABBIT for beam particles and power deposition. The framework is first validated against a tritium-rich, beam-target discharge from the JET DTE2 campaign (#99971). The validated physics parameters are then transposed to predict VNS scenarios. Broad density and beam injection angle scans demonstrate that core beam penetration is highly sensitive to edge density screening. We identify an optimized reference scenario with $n_{e,avg} = 7 \cdot 10^{19}$ part/m^3 and a 179.5° radial NBI inclination that balances a fusion power of 24.1 MW with non-inductive steady-state criteria ($V_{loop} = 1.1$ mV).

Introduction

Evaluating fully integrated components up to Technology Readiness Level (TRL) 8 requires a dedicated nuclear testing facility like the VNS. More information regarding the aim and strategy of this machine can be found in [1], [2], [3]. Global 0.5D models (such as METIS [4]) are highly efficient for initial engineering exploration but rely on pre-defined kinetic profiles and empirical scaling relationships that miss localized non-linear feedback loops. High-fidelity 1.5D modeling is mandatory to capture the tight couplings between current diffusion, magnetic equilibrium, heat/particle transport, and localized auxiliary heating deposition.

In this work, the ASTRA [5] transport code is utilized with a suite of first-principles and advanced analytical submodels, namely TGLF-SAT2 [6] for core turbulent transport analysis, with electromagnetic settings enabled to properly incorporate high-β effects, and RABBIT [7] for self-consistent Neutral Beam Injection (NBI) ion/electron power deposition, fast-ion tracking, and torque calculations. The NEUT module in ASTRA is finally used to compute the neutral tritium gas puff.

*This work is partly supported by the project Piano Nazionale di Ricresa e Resilienza (PNRR) – Next Generation Europe, which has been funded by the European Union and the Italian Ministry of University and Research – DM 118/2023.

This work has been carried out within the framework of the EUROfusion Consortium, funded by the EU via the Euratom Research and Training Programme. The views and opinions expressed herein do not necessarily reflect those of the European Commission.

JET beam-target discharge validation

To evaluate beam-target scenarios typical of the VNS operational mode, the ASTRA framework was first validated against the tritium-rich hybrid H-mode discharge #99971 from the JET DTE2 campaign [8]. This discharge maximized beam-target fusion via pure Deuterium injection into a 15/85 D/T background plasma, yielding a $P_{fus} = 10.1$ MW sustained over a stable > 5s flat-top. This pulse represents the closest experimental analog to a beam-driven VNS core, balancing elevated fusion yield with stable core tungsten concentrations below the radiative collapse threshold. The experimental time traces are available in 1 and Table 1 reports the main 0D parameters of the discharge.

P_{NBI}	29 MW
E_{beam}	108 keV
P_{ICRH}	3.5 MW
$n_{e,avg}$	$4 \cdot 10^{19}$ part/m^3
Z_{eff}	1.8
I_{pl}	2.5 MA
B_T	3.86 T
R/a	3.18
P_{rad}	6/7 MW
P_{fus}	10.1 MW

Table 1: *Main parameters of the JET discharge #99971.*

Kinetic profiles are evolved on the full-radius, with TGLF-

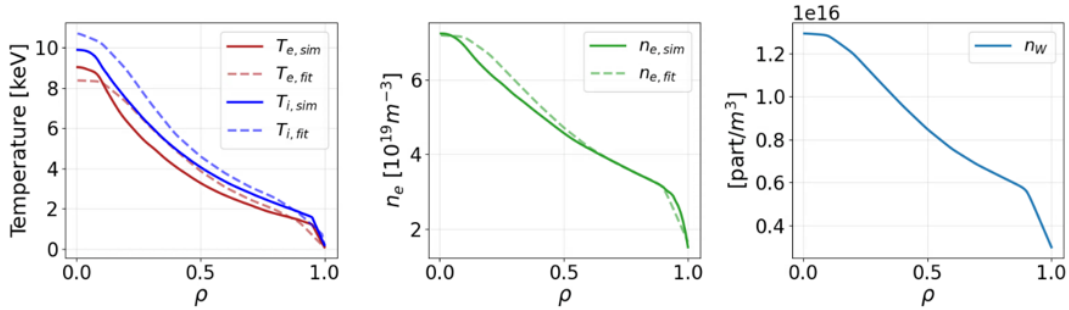

Figure 1: *Fit to experiment (dashed) vs simulated (continuos) profiles of Te,Ti, ne and fixed W density.*

SAT2 domain going until $\rho = 0.95$, and RABBIT modeling the 15-beam injector geometry. In the pedestal region an ad-hoc extra diffusivity for both particle (D_n) and heat (χ_i, χ_e) was added until matching the experimental profiles to mimic the missing turbulence flux. In order to match the radiation (assumed to be mainly due to tungsten accumulation), a profile proportional to the electron density has been fixed, with a concentration across the full-radius of $c_W = 1.8 \cdot 10^{-4}$. This source yielded a result of $P_{rad} = 6.45$ MW, self-consistently computed using analytical radiation rate formula for W as a function of the local electron temperature.

A good agreement with the experimental kinetic profiles was achieved as shown in Figure 1, predicting an overall fusion power of $P_{fus} = 10.8$ MW, establishing a reliable interpretive foundation. To bridge this validation with predictive VNS extrapolations, the added pedestal extra-diffusivity was characterized by an effective transport ratio in the pedestal region of $\chi/D_{eff}{}_{|ped} \sim 3$.

VNS predictive simulations

The validated ASTRA suite was deployed to predict core profiles for the current VNS design, as described in [2]. The primary engineering specifications fixed in the predictive runs are outlined in Table 2.

P_{NBI}	42.5 MW
E_{beam}	120 keV
P_{ECRH}	8 MW
$n_{e,avg}$	$11 \cdot 10^{19}$ part/m^3
Z_{eff}	1.4
I_{pl}	2.5 MA
B_T	5.6 T
R/a	4.25

Table 2: *0D parameters of the current VNS design*

Core turbulent transport within $\rho \leq 0.95$ was handled by TGLF-SAT2, while neoclassical transport was computed across the full radius via analytical formulas. RABBIT modeled a single tangential beam targeting the magnetic axis (R = 2.74 m). The edge transport was constrained using the validated ratio $\chi/D_{eff}{}_{|ped} \sim 3$.

Electron Cyclotron Current Drive (ECCD) was included assuming a driven current of 0.4 MA (for 8 MW of ECRH) with a Gaussian shape localized at $\rho = 0$.

Unlike interpretive setups, the VNS boundary was set to mimic a high-performance scenario operating near the critical pressure limit. Standalone IPED [9] stability calculations determined the maximum allowable pedestal top pressure to be 50 kPa. To implement this constraint, edge temperatures from the pedestal top ($\rho = 0.95$) out to the separatrix were scaled to maintain the 50 kPa threshold, maximizing edge kinetic boundaries. The electron density profile was evolved full-radius under a global line-averaged feedback loop on the average value. In this condition, we are considering the most positive scenario in terms of fusion power produced, maximising the temperature at the pedestal top.

The background plasma composition assumed a Zeff = 1.4, extrapolated from the power exhaust calculation [10], a fixed Helium concentration of $c_{He} = 0.9\%$ (consistent with a fusion power production of $\approx$ 25 MW), and a fixed toroidal velocity profile. The latter was computed using an empirical scaling law derived from high-rotation ASDEX Upgrade (AUG) and JET discharges, which relates NBI-driven torque to induced toroidal velocity while accounting for different plasmas inertia, based on physical assumptions in [11]. Notably, this empirical scaling closely aligns with the Zimmermann momentum transport model [12], which yields similar discharge predictions within the ASTRA framework. Based on the NBI-induced torque calculated for the VNS, the pedestal top and core v_{tor} values were set accordingly on a proportional profile.

The application of RABBIT in the initial ASTRA predictive runs, testing the above-mentioned scenario derived from the 0.5D METIS projections with $n_{e,avg} = 11 \cdot 10^{19}\ part/m^3$, uncovered a severe edge density screening effect. High edge density rapidly ionized the incoming 120 keV neutral beams near the plasma periphery, trapping beam deposition at $\rho > 0.7$. This lack of core beam penetration collapsed central temperatures and restricted the fusion power to just $\approx$ 17 MW.

To restore beam penetration, a density scan was executed. Lowering the line-averaged target to $n_{e,avg} = 7 \cdot 10^{19}\ part/m^3$ was found to optimize beam penetration without over-diluting or distorting the edge D/T fuel mixture. To maximize even more the performance within engineering margins, an optimization scan was conducted by varying NBI beam energy (120-150 keV), ECRH power (8-10 MW), and the NB injection radial location (from $R = 2.74$ m to a more radial at $R = 2.05$ m). The matrix of configurations is sum-

Case	Angle [°]	P_{NBI} [MW]	E_{NBI} [keV]	P_{ECRH} [MW]	P_{fus} [MW]	V_{loop} [mV]	Rot loss [MW]	$V_{tor,0}$ [km/s]
Design	180	42.5	120	8	**16.80**	**14**	8.73	740
150 keV	180	42.5	**150**	**10**	**21.54**	**-10**	8.10	665
-0.5 deg	**179.5**	42.5	**150**	**10**	**24.11**	**1.1**	7.72	646
-1 deg	**179**	42.5	**150**	**10**	**28.62**	**10**	7.07	620
-2 deg	**178**	42.5	**150**	**10**	**32.05**	**18**	5.7	550

Table 3: *Input parameters and key outputs from the VNS optimization scan.*

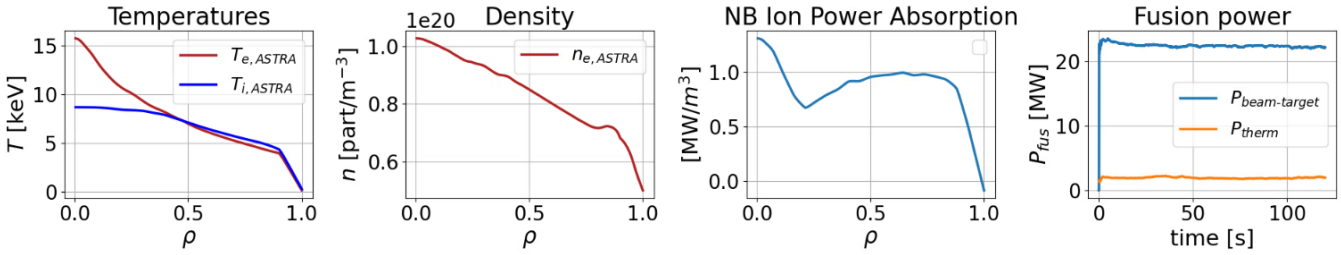

Figure 2: *From left to right: T_e, T_i, n_e radial profiles, NBI power deposition profile, time evolution of fusion power fractions.*

marized in Table 3.

Steady-state operation targets require the loop voltage (V_{loop}) to remain below 2 mV to guarantee a continuous pulse within the available flux of 2 Wb at the flat top. Shifting the NBI alignment toward a more radial trajectory reduces the core toroidal velocity (v_{tor}) profile, effectively lowering the momentum fraction transformed into plasma rotation. While this mechanical torque input is not a traditional loss channel, a critical physics effect emerges at high rotation velocities: because the plasma rotates in the same direction as the co-injected neutral beams, the relative impact energy in the center-of-mass frame is strongly reduced, consequently degrading the beam-target fusion power yield.

As a consequence, while more radial injection angles maximize the core geometric path length and increase raw thermonuclear reactivity, they suppress the beam-driven current density. This trade-off explains why higher fusion powers correlate with an unsustainable rise in inductive loop voltage. To maintain steady-state compatibility, the -0.5° radial inclination case was selected as the reference configuration; it represents the tightest operational compromise, restricting V_{loop} to a stable 1.1 mV despite being far from the $P_{fus} \approx 38$ MW targeted to reach the NWL = 0.5 MW/m^2.

The comprehensive 1.5D profiles for this reference scenario are illustrated in Figure 2. The self-consistently modeled 150 keV neutral beam successfully overcomes the edge density screening barrier, providing targeted core power deposition that peaks inside $\rho < 0.2$ (Fig. 3c). This highly localized core heating sustains a strongly peaked electron temperature profile, significantly decoupling from the ion temperature (Fig. 3a). Combined with a self-consistent, peaked electron density distribution (Fig. 3b) ($n_{e,avg} = 7 \cdot 10^{19}\ part/m^3$) that optimizes the core D/T fuel mix, this framework yields 24.1 MW of fusion power. Ultimately, the complex interplay between core beam penetration, localized current drive alignment, and loop voltage constraints confirms this configuration as the most physically viable operating window within current VNS machine limits.

Conclusion and further studies

An integrated 1.5D ASTRA-TGLF-RABBIT framework was validated against JET DTE2 hybrid discharge #99971. Transposing this framework to predictive VNS modeling revealed that design target of $n_e = 11 \cdot 10^{19}\ part/m^3$ suffers from strong edge density screening, preventing NBI penetration. Extensive parametric scans identified an optimized reference scenario at $7 \cdot 10^{19}\ part/m^3$ paired with a 179.5° radial NBI injection angle, maximizing core beam penetration to yield 24.1 MW of fusion power while satisfying steady-state non-inductive criteria ($V_{loop} = 1.1\ mV$).

This scenario highlights critical trade-offs: lower core densities shrink separatrix (n_{sep}) and pedestal margins, potentially challenging edge exhaust detachment. Furthermore, high co-injection torque enhances adverse neoclassical W transport accumulation and decreases beam impact energy, while radial injection angles reduce the non-inductive current fraction, requiring on-axis ECCD compensation.

Future studies will assess robustness against operational uncertainties and core impurity accumulation (W and Z_{eff}). Subsequent iterations will evaluate compatibility with edge exhaust, q-profiles, MHD stability, and energetic particle modes. Given these trade-offs, multi-parameter design explorations using METIS coupled to MADE [13] verified against these ASTRA-RABBIT-TGLF results will be deployed to revise the VNS actual design point in terms of machine and auxiliary systems geometry and settings.

References

[1] G. Federici et al., *Nuclear Fusion*, vol. 63, no. 12, p. 125 002, 2023.

[2] C. Bachmann et al., *Nuclear Fusion*, vol. 66, no. 4, p. 046 015, 2026.

[3] M. Siccinio et al., this conference, 2026.

[4] J. F. Artaud et al., *Nuclear Fusion*, vol. 58, no. 10, p. 105 001, 2018.

[5] G. Tardini et al., *Plasma Physics and Controlled Fusion*, vol. 68, no. 6, p. 065 024, 2026.

[6] G. M. Staebler et al., *Plasma Physics and Controlled Fusion*, vol. 63, no. 1, p. 015 013, 2020.

[7] M. Weiland et al., *Nuclear Fusion*, vol. 58, no. 8, p. 082 032, 2018.

[8] M. Maslov et al., *Nuclear Fusion*, vol. 63, no. 11, p. 112 002, 2023.

[9] M. G. Dunne et al., *Plasma Physics and Controlled Fusion*, vol. 59, no. 1, p. 014 017, 2016.

[10] S. Wiesen et al., in *Conference Pre-print*, Pre-print draft, 30 September 2025, 2025.

[11] P. C. de Vries et al., *Nuclear Fusion*, vol. 48, no. 6, p. 065 006, 2008.

[12] C. F. B. Zimmermann et al., *Physics of Plasmas*, vol. 31, no. 4, p. 042 306, 2024.

[13] L. Giannini et al., *Fusion Engineering and Design*, vol. 193, p. 113 659, 2023. DOI: 10.1016/j.fusengdes.2023.113659.